

Coexistence of Two 1:1 Complexes of Oxyphenonium Bromide and α-Cyclodextrin

Noriaki Funasaki,* Hiroshi Yamaguchi, Seiji Ishikawa, and Saburo Neya

Kyoto Pharmaceutical University, Misasagi, Yamashina-ku, Kyoto 607-8414

(Received January 18, 2002)

The complexation of 2-(2-cyclohexyl-2-hydroxy-2-phenylacetoxy)-*N*,*N*-diethyl-*N*-methylethanaminium bromide (oxyphenonium bromide, OB) and α-cyclodextrin (α-CD) in deuterium oxide was investigated by 500 MHz proton NMR spectroscopy, molecular mechanics, and molecular surface-area calculations. The ROESY spectrum revealed that two 1:1 complexes of OB and α-CD, the phenyl-in complex and the cyclohexyl-in complex, coexist simultaneously. The ROE intensities of intermolecular cross-peaks and molecular-mechanics calculations provided the structures of these complexes. The ROE intensities were well-correlated with the effective inter-proton distances for the estimated structures. The observed binding constant (70 $dm^3\ mol^{-1}$) was close to the sum of the binding constants of α-CD with phenol and cyclohexanol. This agreement supported the coexistence of the two complexes, and allowed us to estimate the mole fraction of the phenyl-in complex of 0.3. The chemical shift variations ($\Delta\delta_{OB-CD}$) at full binding for aromatic protons of OB are smaller than those of the benzenesulfonate–α-CD complex. Their ratio gave another estimate of the phenyl-in complex mole fraction (0.38). The averaged structure of OB in the two complexes was estimated from a comparison between the observed and theoretical shifts for four pairs of cyclohexyl protons; the phenyl and cyclohexyl groups in the complexes are slightly more distant than those in the free state. The structures of the phenyl-in complex and the cyclohexyl-in complex, estimated by hydrophobic molecular surface-area calculations, predicted binding constants closer to the observed ones than those by molecular-mechanics calculations.

Cyclodextrins (CDs) have homogeneous toroidal structures of different molecular size; most typical are cyclohexaamylose (α-CD), cycloheptaamylose (β-CD), and cyclooctaamylose (γ-CD). The toroidal structure has a hydrophilic surface, making it water soluble, whereas the cavity is composed of methine hydrogens, giving it a hydrophobic character. As a consequence, the CDs can include other hydrophobic molecules of appropriate dimensions and shapes.[1,2]

Very recently, we studied the suppression of the bitter taste of oxyphenonium bromide (OB), an antiacetylcholine drug, by CDs, and showed that this suppression can be predicted based on ultraviolet (UV) spectroscopic and electromotive force data.[3,4] Although UV data suggested that OB penetrates shallowly into the α-CD cavity,[3] this estimation should be confirmed by NMR. Electromotive force data indicated the 1:1 stoichiometry of OB and α-CD.[4] As Fig. 1 shows, OB has phenyl and cyclohexyl groups. These groups can bind to the cavities of the CDs. There are two plausible 1:1 complexes of OB and α-CD. We determined the solution structure of OB by proton NMR spectroscopy and molecular-mechanics calculations.[5] This structure of OB may be changed by α-CD inclusion.

The guest molecule that has two binding sites for CD can generally form one or two kinds of the 1:1 complex and the 1:2 complex. Because the complexation of the CD and the guest is usually rapid on the NMR time scale, the NMR spectrum usually gives information averaged over all species present in the system.[6–8] At 223 K in *N*,*N*-dimethylformamide, however, 1:1 and 1:2 complexes of acenaphthene and β-CD gave separate signals on the NMR spectra.[9] Because electron spin resonance (ESR) spectroscopy has a shorter time scale (ca. 10^6 Hz), the complexed and uncomplexed species of a paramagnetic guest can provide distinct signals on the ESR spectrum. For instance, when the *t*-butyl(diphenylmethyl)ami-

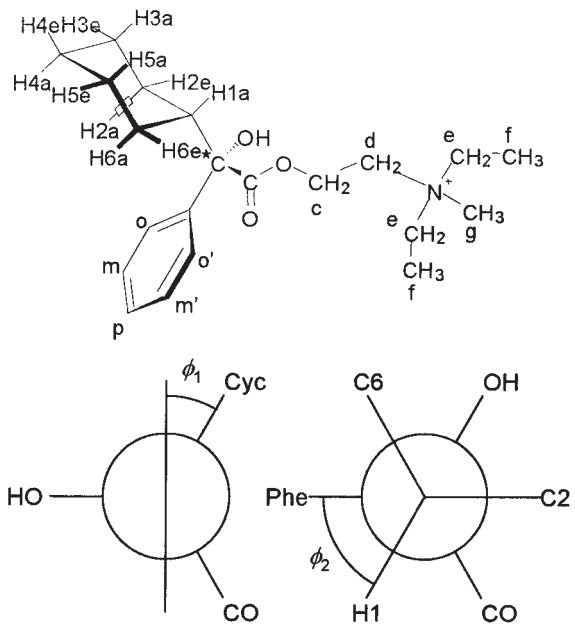

Fig. 1. Chemical structures of oxyphenonium bromide and the definition of dihedral angles around the C1–C* and C(phenyl)–C* bond axes of *S*-OB in the Newman projection.

nyl oxide radical is complexed by β-CD in water, either the phenyl group or the *t*-butyl group can be included, and the binding constants for these groups can be determined.[10,11] Bimodal 1:1 complexes of a naphthalene derivative with a modified β-CD have been detected by time-resolved fluorescence spectroscopy.[12] These ESR and fluorescence methods, however, do not provide any information on the detailed structure of the complex. Furthermore, for bimodal 1:1 complexes, the observed macroscopic binding constant consists of two microscopic binding constants and their relative magnitude has attracted strong interest.[8,13–15]

In this work, we investigated the complexation of OB and α-CD in water by NMR, and showed that two 1:1 complexes coexist. The structures of these complexes were estimated from molecular-mechanics and molecular surface areas. The structural changes of OB with α-CD inclusion, the populations of these complexes, and the microscopic binding constants will also be discussed.

Experimental

Materials. Commercial samples of 99% deuterium oxide (Aldrich) and a racemic mixture of *R*- and *S*-OB (Sigma) were used as received. This sample of OB gave a single peak on a reversed-phase high-performance liquid chromatogram. Tetramethylammonium chloride (Nacalai Tesque, Kyoto) was of guaranteed grade.

NMR Measurements. All NMR experiments were carried out in deuterium oxide at 309.7 ± 0.1 K. This temperature was chosen for a comparison with our experiments connecting the bitter taste of OB.[3,4] The proton chemical shifts of OB and α-CD were determined for a series of 2 mmol dm^{-3} (mM) α-CD solutions containing OB in the concentration range of 0.5 mM to 20 mM. The proton chemical shifts (δ) were referenced to the internal signal of tetramethylammonium chloride at $\delta = 3.176$ ppm.[16] This standard value was determined with reference to external sodium 4,4-dimethyl-4-silapentane-1-sulfonate in D_2O. The precision of the chemical shift is 0.001 ppm. The ^{1}H NMR spectra were obtained with a JEOL Lambda 500 spectrometer at 500 MHz, and the data processing was performed with standard software. All of the obtained one-dimensional spectra were deconvoluted with Nuts NMR data-processing software (Acorn NMR Inc.) in order to determine the chemical shifts and spin-spin coupling constants. The chemical shift induced by the benzene ring was theoretically calculated with our own software.[5]

Two-dimensional rotating-framework Overhauser enhancement spectroscopy (ROESY) for a solution containing 40 mM OB and 40 mM α-CD was performed at 500 MHz with the JEOL standard pulse sequences; the data consisted of 8 transients collected over 2048 complex points. A mixing time of 400 ms, a repetition delay of 1.2 s, and a 90° pulse width of 11.0 μs were used. The ROESY data set was processed by applying a Gaussian function in both dimensions and zero-filling to 2048 × 2048 real data points prior to a Fourier transformation. Small cross-peaks were neglected, because their magnitude was close to that of the noise. The volume of a cross-peak was determined with our own software.

Molecular Mechanics Calculations. The solution structure of OB, determined by NMR, was employed.[5] The structure of α-CD in the crystal structure of the 1:1 complex of α-CD and benzenesulfonate was employed.[17] This structure of α-CD was regarded as being a rigid body, whereas that of OB was regarded as being flexible. The starting structure of the complex of OB and α-CD was generated based on NMR data with our own software,[8,18] and energy minimization of this structure was carried out by molecular-mechanics calculations. These calculations were performed with a Molecular Simulation Insight II/Discover (98.0) on a Silicon Graphics Octane workstation. The Discover III CVFF force field was used for energy minimization.[19] The energy minimization was performed using the conjugate gradients method to a derivative of 0.001 kcal mol^{-1} with a cut-off distance for van der Waals' and electrostatic forces of 1.6 nm.

The complex was placed into a unit cell of 2.5 × 2.5 × 3.5 nm, where the symmetry axis of α-CD was parallel to the long axis. The complex was then soaked in 642 water molecules. A periodic boundary condition was applied on this cell. The total potential energy of this system was minimized. Simulated annealing of the system was carried out every 1 fs for 1000 fs at a final temperature of 500 K in the *NVT* ensemble, after the initial velocities of the atoms were given at 10 K. After a molecular-dynamics simulation, the total potential energy of this system was again minimized to obtain the final structure of the complex.

Calculations of the Molecular Surface Areas. As already reported,[18] the Bondi radii (r) were employed for calculations of water-accessible molecular surface area (r_H(aliphatic) = 0.120 nm, r_H(aromatic) = 0.100 nm, r_O(ether) = 0.152 nm, r_O(carbonyl) = 0.150 nm, r_C (aromatic) = 0.177 nm, r_C(aliphatic) = 0.170 nm, and r_N (aliphatic) = 0.155 nm).[20] A water radius of $r_W = 0.14$ nm was employed for calculations of the water-accessible molecular surface areas. The groups of carbonyl, hydroxy, ether oxygen, and ammonium nitrogen of OB and α-CD were regarded as being hydrophilic groups, and the other groups were regarded as hydrophobic groups. All atomic surface areas were calculated, and then from a summation of these areas over the hydrophobic and hydrophilic groups, the hydrophobic and hydrophilic areas (A_o and A_w), were calculated, respectively. Because two chemically nonbonded atoms cannot approach within their Bondi radii, such structures were regarded as being unstable.

Results

Chemical Shifts. Figure 2 shows a 500 MHz proton NMR spectrum of a mixture of OB ($C_{OB} = 4$ mM) and α-CD ($C_{CD} = 2$ mM). The assignments of all the protons of OB[5] and α-CD[21,22] have already been established. α-CD (CD) consists of six kinds of carbon atoms (C1–C6). The chemical shift

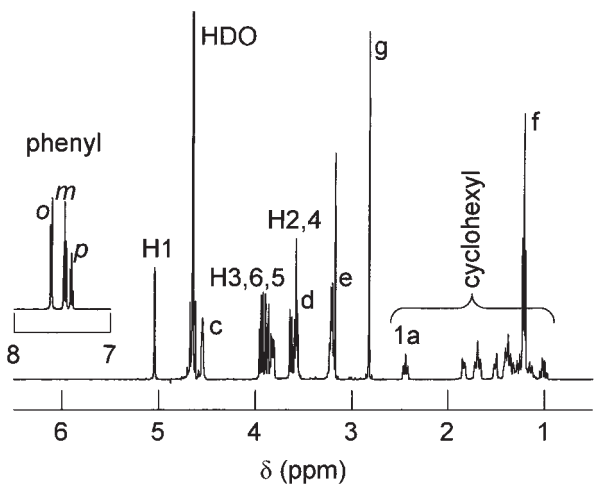

Fig. 2. Proton NMR spectrum of a mixture of OB ($C_{OB} = 4$ mM) and α-CD ($C_{CD} = 2$ mM).

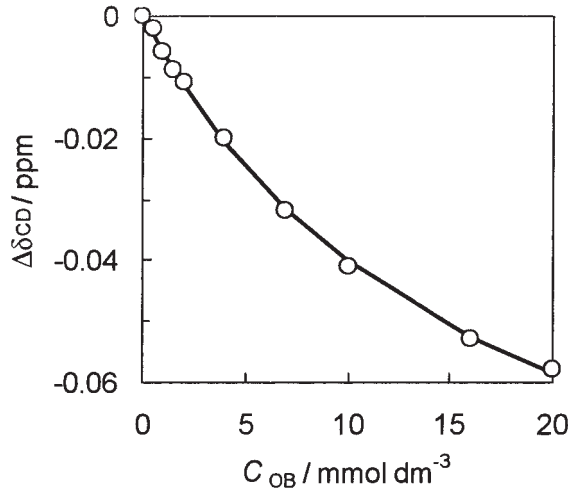

Fig. 3. Dependence of the chemical shift of proton H3 of α-CD ($C_{CD} = 2$ mM) on the OB concentration. The solid line is calculated using the values of K_1 and $\Delta\delta_{CD}$ (H3) shown in Tables 1 and 2.

of the H3 proton bonded to the C3 atom exhibits the largest variation among those of all the protons, and is shown as a function of the OB concentration in Fig. 3. This variation is induced by the 1:1 complexation of these compounds, because the absence of other complexes was established by electromotive force measurements.[4]

When this complexation is rapid on the NMR time scale, the observed chemical shift of an OB proton can be written as

$$\delta = ([OB]\delta_{OB} + [OB\text{–}CD]\delta_{OB\text{–}CD})/C_{OB}. \quad (1)$$

Here, [OB] and [OB–CD] denote the concentrations of the free OB molecule and the 1:1 complex, respectively, and C_{OB} denotes the total concentration of the free and bound species of OB; δ_{OB} and $\delta_{OB\text{–}CD}$ stand for the chemical shifts of these species. The observed chemical shift of an α-CD proton can be written as

$$\delta = ([CD]\delta_{CD} + [OB\text{–}CD]\delta_{OB\text{–}CD})/C_{CD}. \quad (2)$$

Here, [CD] and C_{CD} denote the concentration of the free CD molecule and the total concentration of the free and bound species of α-CD, respectively, and $\delta_{OB\text{–}CD}$ stands for the chemical shift of the bound CD molecule. Using the equilibrium constant (K_1) of this complexation, one can write the concentrations of these species as follows:

$$[OB] = \{K_1C_{OB} - K_1C_{CD} - 1 + [(K_1C_{OB} - K_1C_{CD} - 1)^2 + 4K_1C_{OB}]^{1/2}\}/2K_1, \quad (3)$$

$$[OB\text{–}CD] = \{K_1C_{OB} + K_1C_{CD} + 1 - [(K_1C_{OB} - K_1C_{CD} - 1)^2 + 4K_1C_{OB}]^{1/2}\}/2K_1, \quad (4)$$

$$[CD] = \{K_1C_{CD} - K_1C_{OB} - 1 + [(K_1C_{OB} - K_1C_{CD} - 1)^2 + 4K_1C_{OB}]^{1/2}\}/2K_1. \quad (5)$$

Regarding K_1 and $\delta_{OB\text{–}CD}$ as adjustable parameters, one can calculate the theoretical chemical shift of an α-CD proton at a given set of C_{OB} and C_{CD} from Eqs. 2–5 by a nonlinear least-squares method. Thus, we determined the best-fit values of these parameters from the observed $\Delta\delta$ values of H3 (Fig. 3). These $\delta_{OB\text{–}CD}$ and K_1 values and standard deviations are given in Tables 1 ($\Delta\delta_{OB\text{–}CD} = \delta_{OB\text{–}CD} - \delta_{OB}$ or $= \delta_{OB\text{–}CD} - \delta_{CD}$) and 2.

The binding constant of OB and α-CD had already been determined in 154 mM sodium bromide solutions at 309.7 K by electromotive-force measurements[4] and UV spectroscopy.[3] As shown in Table 2, these binding constants are close to that obtained in this work. This fact indicates that the present K_1 value is reliable. Thus, by using this K_1 value, we determined the best-fit $\Delta\delta_{OB\text{–}CD}$ values and the standard deviations for all protons of OB and α-CD, except for H3; those values for the protons of the phenyl and cyclohexyl groups of OB and α-CD are given in Table 1. From the magnitude of the $\Delta\delta_{OB\text{–}CD}$ values, one can imagine the structure of the complex: OB is shallowly incorporated from the wider rim (the secondary alcoholic side) of the α-CD cavity, and the cyclohexyl group of OB is incorporated. In Table 2 the literature binding constants (K_1) of α-CD with cyclohexanol and phenol are also summarized.

ROESY Spectrum. To confirm the structure estimated from the chemical-shift variations, we recorded the ROESY spectrum. As Figs. 4 and 5 show, OB and α-CD exhibit intermolecular cross-peaks. The ROE intensities of the cross-peaks between the protons (H3, H5, and H6) of α-CD and the phenyl and cyclohexyl protons of OB are summarized in Table 3. Based on electrochemical data we showed that OB and α-CD form the 1:1 complex alone.[4] In addition to the NMR data, we have UV spectroscopic evidence that the phenyl group of OB penetrates into the α-CD cavity.[4] These results indicate that both of the phenyl and cyclohexyl groups are incorporated in the α-CD cavity to form two kinds of 1:1 complexes, the cyclohexyl-in complex ($OB\text{–}CD_C$) and the phenyl-in complex ($OB\text{–}CD_P$).

The volume (ROE intensity) of the cross-peak was determined by integration. The ROE intensity of the cross peak is proportional to the number of equivalent protons. When internal rotations of a molecule are slower than the overall tumbling, we can expect the following relation:[24,25]

$$ROE = k\sum_{i=1}^{n_{CD}}\sum_{j=1}^{n_{OB}} d_{CDiOBj}{}^{-6}. \quad (6)$$

Here, d_{CDiOBj} denotes the distance between a proton (CDi) of CD and a proton (OBj) of OB, and n_{CD} and n_{OB} stand for the number of equivalent protons of the α-CD and OB group, respectively. For simplicity, the effective distance (d_{eff}) is defined as

$$(d_{eff})^{-6} = (1/n_{CD}n_{OB})\sum_{i=1}^{n_{CD}}\sum_{j=1}^{n_{OB}} d_{CDiOBj}{}^{-6}. \quad (7)$$

From Eqs. 6 and 7 we can expect that $ROE/n_{CD}n_{OB}$ increases as two protons become closer to each other.

In Table 3, $ROE/n_{CD}n_{OB}$ is shown for intermolecular cross-peaks. Because there is no cross-peak between H1 and the protons of OB, the H1 region was omitted from Figs. 4 and 5 and Table 3. Because the H3 and H6*S* protons of α-CD overlapped with each other in the ROESY spectrum (Figs. 4

Table 1. Chemical Shifts of Free OB and α-CD and Chemical Shift Variations Induced by Complexation with OB, Benzenesulfonate (BS), and Cyclohexanol (cHexOH)

Proton	δ_{free}	$\Delta\delta_{OB-CD}$	$\Delta\delta_{complex}$(BS)[a]	$\Delta\delta_{complex}$(cHexOH)[b]
H1	5.051	-0.017 ± 0.001[c]	-0.032	0.00
H2	3.632	0.007 ± 0.001	-0.068	0.01
H3	3.976	-0.100 ± 0.003	-0.204	-0.02
H4	3.581	-0.007 ± 0.001	-0.035	0.00
H5	3.832	-0.064 ± 0.001	0.014	-0.03
H6	3.885	-0.013 ± 0.001	0.019	-0.01
Ho	7.611	0.054 ± 0.004	0.211	—
Hm	7.469	0.077 ± 0.004	0.131	—
Hp	7.405	0.027 ± 0.004	0.073	—
H1a	2.437	0.077 ± 0.004	—	0.06
H2a	1.380	0.117 ± 0.004	—	0.09
H2e	1.497	0.124 ± 0.004	—	0.10
H3a	1.331	0.125 ± 0.004	—	0.07
H3e	1.823	0.195 ± 0.004	—	0.07
H4a	1.135	0.144 ± 0.004	—	0.06
H4e	1.672	0.096 ± 0.004	—	0.08
H5a	1.258	0.160 ± 0.004	—	0.07
H5e	1.689	0.244 ± 0.004	—	0.07
H6a	1.003	0.112 ± 0.004	—	0.09
H6e	1.382	0.207 ± 0.004	—	0.10

a) The data for the complex of sodium benzenesulfonate and α-CD at full binding, taken from Ref. 26. b) Observed $\Delta\delta_{complex}$ values taken from Ref. 27, where the molar ratios of cyclohexanol to α-CD are 0.48 for the α-CD protons and 1.06 for the cyclohexanol protons. Because these are $\Delta\delta_{complex}$ values at partial binding for cyclohexanol, relative values alone have physical meaning. c) Standard deviation.

Table 2. Observed and Theoretical Binding Constants of α-CD with OB, Phenol, and Cyclohexanol[a]

Guest	K_1/dm^3 mol^{-1}
OB	70 ± 4 (NMR, 308 K),[b] 94 (UV, 308 K),[c] 58 (EMF, 308 K)[d]
Phenol	37,[e] 20.7,[f] 20.0,[g] 16000,[h] 18.9,[i] 0,[j] 19.8 (308 K)[f]
Cyclohexanol	62,[f] 58,[k] 64.6,[l] 14790,[m] 56 (308 K),[f] 50 (308 K)[k]

a) At 298 K, unless specified. b) This work (SD = 4.0). c) Determined in a 154 mM sodium bromide solution by UV, taken from Ref. 3. d) Determined in a 154 mM sodium bromide solution by electromotive force measurements, taken from Ref. 4. e) Taken from Ref. 31. f) Taken from Ref. 32. g) Taken from Ref. 33. h) Taken from Ref. 34. i) Taken from Ref. 35. j) Taken from Ref. 36. k) Taken from Ref. 27. l) Taken from Ref. 37. m) Taken from Ref. 38.

and 5), these protons were regarded as being equivalent: $n_{CD}(H36S) = 12$. Similarly, because three protons (H2a, H3a, and H6e) of OB overlapped with one another, they were dealt with as equivalent ones: $n_{OB}(H2a3a6e) = 3$.

The magnitude of the cross-peaks for the phenyl protons is slightly smaller than that for the cyclohexyl protons. This indicates that a mole of the phenyl-in complex is smaller than a mole of the cyclohexyl-in complex.

Structures of Complexes. To estimate the structures of these two complexes, we must take into consideration two microequilibria of these simultaneous complexations:

$$\mathrm{OB} + \mathrm{CD} \overset{K_{1C}}{=} \mathrm{OB{-}CD_C}, \tag{8}$$

$$\mathrm{OB} + \mathrm{CD} \overset{K_{1P}}{=} \mathrm{OB{-}CD_P}. \tag{9}$$

The sum of these microscopic equilibrium constants must be equal to the macroscopic constant (K_1).[14,15,23] The chemical shift of the complex consists of the contributions of the two complexes

$$\delta_{OB-CD} = (K_{1C}\delta_{OB-CDC} + K_{1P}\delta_{OB-CDP})/K_1. \tag{10}$$

Here, δ_{OB-CDC} and δ_{OB-CDP} denote the chemical shifts of the two complexes, respectively. From Eq. 10 we can write the chemical-shift variation with this complexation as

$$\Delta\delta_{OB-CD} = (K_{1C}\Delta\delta_{OB-CDC} + K_{1P}\Delta\delta_{OB-CDP})/K_1. \tag{11}$$

Thus, the observed chemical shift variation comes from the two complexations. If K_{1C} and K_{1P} are determined, the mole fractions of these species in the 1:1 complex can be calculated from K_{1C}/K_1 and K_{1P}/K_1.

Keeping this consideration in mind, we compared the chemical-shift variations of OB with those of sodium benzenesulfonate (BS).[26] The $\Delta\delta_{OB-CD}$ values for the aromatic protons of OB are much smaller than those for BS, as shown in Table 1. This result is consistent with the partial incorporation of the phenyl group of OB, because the $\Delta\delta_{OB-CD}$ values for the aro-

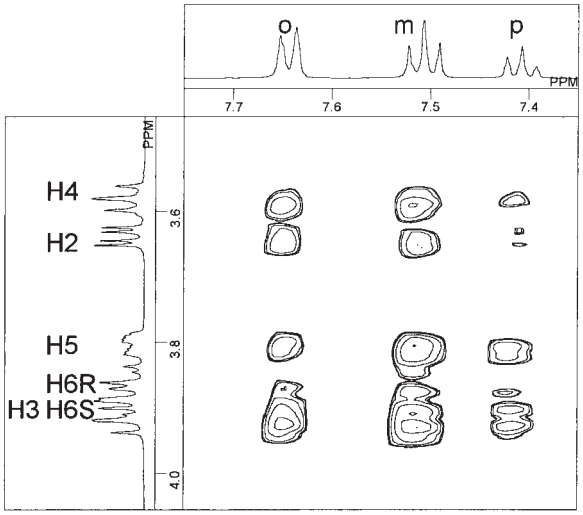

Fig. 4. Partial ROESY spectrum of a mixture of OB ($C_{OB} = 40$ mM) and α-CD ($C_{CD} = 40$ mM) in the benzene region.

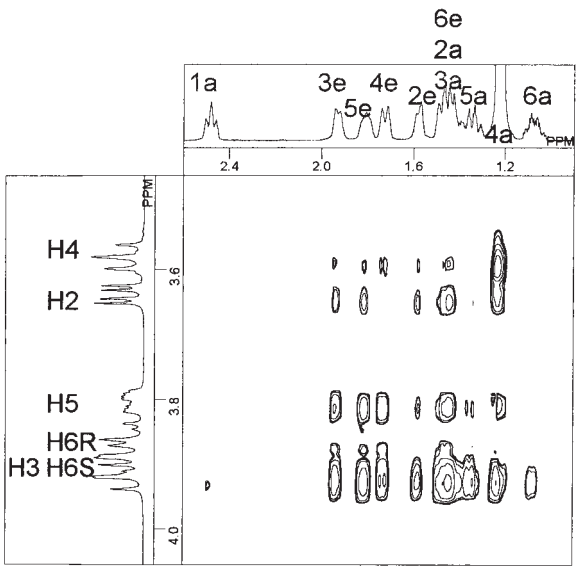

Fig. 5. Partial ROESY spectrum of a mixture of OB ($C_{OB} = 40$ mM) and α-CD ($C_{CD} = 40$ mM) in the cyclohexane region.

Table 3. ROESY Intensities $ROE/n_{CD}n_{OB}$ of Intermolecular Cross-Peaks between the Protons of the Phenyl and Cyclohexyl Groups of OB and the H3, H5, H6*S*, and H6*R* Protons of α-CD in a 500 MHz ROESY Spectrum[a)]

CD	OB											
	1a	2a,3a,6e	2e	3e	4a	4e	5a	5e	6a	o	m	p
H3,6*S*	0	12.1	7.2	12.6	13.9	9.1	8.4	14.1	1.7	6.0	9.9	2.5
H5	0	3.0	0.4	9.5	3.9	10.5	0.3	7.3	0	2.1	8.6	4.3
H6*R*	0	0.4	0	0.8	0	1.4	0	0.7	0	0.4	1.7	0.1

a) Recorded for the solution containing 40 mM OB and 40 mM α-CD.

matic protons would be close to zero for the cyclohexyl-in complex ($\Delta\delta_{OB-CDC} = 0$) and to those of the BS complex for the phenyl-in complex in Eq. 11, respectively. The $\Delta\delta_{OB-CD}$ values for most of the CD protons in an OB–CD complex are smaller than those in a BS–CD complex. The $\Delta\delta_{OB-CD}$ values of the CD protons for the phenyl-in complex should generally be larger than those for the cyclohexyl-in complex, because the phenyl group has larger magnetic effects on the neighboring atoms than the cyclohexyl group. The $\Delta\delta_{OB-CD}$ value for proton H5 of CD in the OB–CD complex is negative. This sign is consistent with that of the α-CD–cyclohexanol (cHexOH) complex, but is opposite to that of the BS–CD complex; for the $\Delta\delta_{OB-CD}$ value of proton H5 of CD in the CD–OB complex, the cyclohexyl-in complex would make a larger contribution than the phenyl-in complex. Protons H3 and H5 of CD are close to proton H4e of OB (Table 3). As shown in Table 1, the incorporation of cyclohexanol into the α-CD cavity induces downfield shifts of the cyclohexyl protons.[27] However, because these $\Delta\delta_{complex}$ (cHexOH) values are at a partial binding, they are smaller than those of OB.

Based on these chemical shifts (Table 1) and NOE data (Table 3 and Figs. 4 and 5), we can imagine rough structures of the phenyl-in and cyclohexyl-in complexes. The structures of OB in the free state and α-CD in the BS–α-CD complex were used as initial structures,[26] and the energy-minimized structures of the complexes were estimated by molecular mechanics (MM). These structures are shown in Fig. 6. The dihedral angles (φ_1 and φ_2) of OB around the C(phenyl)–C* and C1–C* bond axes of OB in the complexes are shown in Table 4.

Based on these MM structures, we calculated the effective distance (d_{eff}) and plotted it against the ROE intensity (*ROE*/

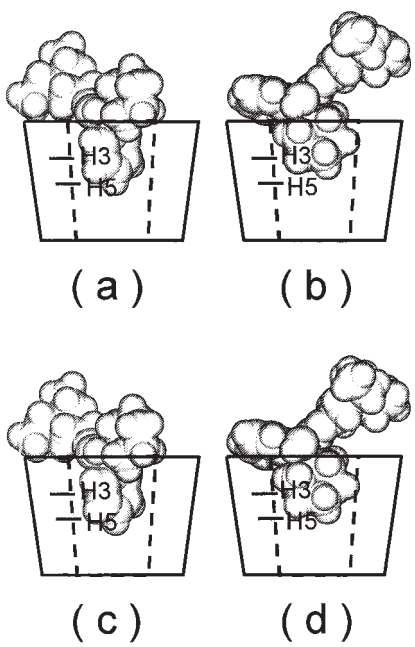

Fig. 6. Three-dimensional structures of (a) the phenyl-in complex and (b) the cyclohexyl-in complex estimated by molecular mechanics and (c) the phenyl-in complex and (d) the cyclohexyl-in complex estimated by molecular surface area calculations.

Table 4. Structures and Binding Constants of Cyclohexyl-in and Phenyl-in Complexes Estimated on the Basis of Molecular Mechanics (MM) and Molecular Surface Areas (SA)

Structure	x	φ_1	φ_2	ΔA_{oo}	K_1
	nm	degree	degree	nm^2 $molecule^{-1}$	dm^3 mol^{-1}
Phenyl-in by MM	0	−76	65	1.80	16.4
Cyclohexyl-in by MM	0	−59	56	1.73	12.4
Phenyl-in by SA	−0.05	−76	65	1.83	18.8
Cyclohexyl-in by SA	−0.11	−59	56	1.96	31.9

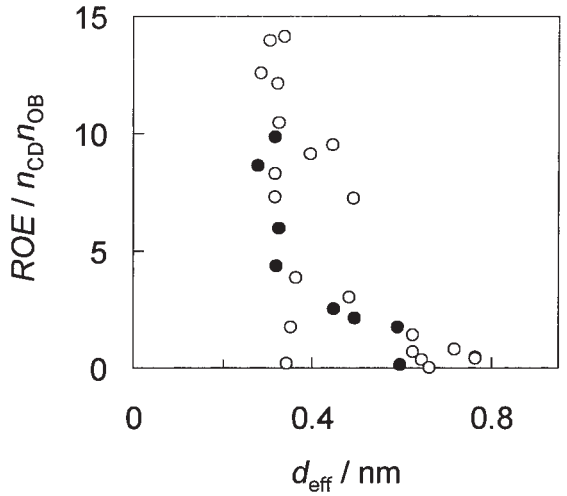

Fig. 7. The observed $ROE/n_{CD}n_{OB}$ values plotted against the effective proton–proton distances calculated for the phenyl protons (closed circles) of the phenyl-in complex and the cyclohexyl protons (open circles) of the cyclohexyl-in complex in the energy-optimized structures.

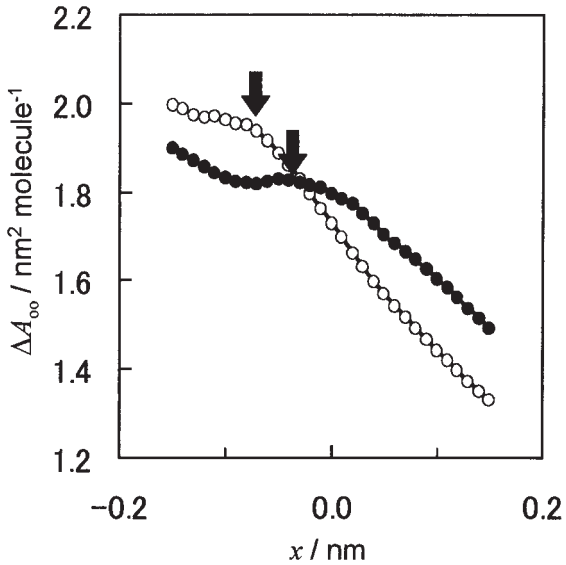

Fig. 8. ΔA_{oo} values plotted against the penetration depth of the phenyl group (closed circles) and the cyclohexyl group (open circles) in the α-CD cavity, where the arrows correspond to the structures of the complexes estimated by molecular surface areas and the depth of $x = 0$ denotes the molecular mechanics structure.

$n_{CD}n_{OB}$). As expected from Eqs. 6 and 7, $ROE/n_{CD}n_{OB}$ decreased with increasing d_{eff} (Fig. 7). This finding indicates that the structures of the phenyl-in and cyclohexyl-in complexes are reasonable. Some scatter in Fig. 7 can be ascribed to the dependence of the ROE intensity on the experimental conditions and the internal motion of the complexes.

In the complex of OB and α-CD, the hydrophobic groups of OB would likely to be in more contact with the hydrophobic groups of α-CD, and in less contact with the hydrophilic groups of α-CD. The same thing holds true for α-CD. We have recently proposed a molecular surface-area method for predicting the structure and binding constant of complexation.[18] Among the decreases in the molecular surface area with docking of the host and guest, the ΔA_{oo} value is the most important area. This is the decrease in the area of contact between the hydrophobic surfaces of the host and guest in the complex, and may be termed the matching hydrophobic surface area decrease. The structure of the complex at the maximum ΔA_{oo} value is the most stable, which is well correlated with the binding constant.

Figure 8 shows this ΔA_{oo} value as a function of the penetration depth (x) for the phenyl-in and cyclohexyl-in complexes into the symmetric axis of α-CD, while the structure of OB and α-CD were kept rigid. The structures of OB and that of α-CD, determined by NMR[5] and X-ray crystallography,[17] were used. In Fig. 8 a penetration depth of $x = 0$ is the position for the structures (Figs. 6a and b) of the complexes estimated by molecular mechanics. The ΔA_{oo} value increases with a deeper penetration of the phenyl and cyclohexyl groups, and the complexes become more stable in the free energy of hydrophobic interactions. However, OB and α-CD are in van der Waals contact at the depth shown by the arrows. As OB and α-CD approach beyond this depth, the energy of the van der Waals repulsion increases rapidly. Therefore, we regarded the structures being in van der Waals contact as the most stable. Table 4 shows the penetration depth and the ΔA_{oo} value for these stable structures shown in Figs. 6c and d.

Because x is rather small, the SA structures are close to the MM structures. This indicates that the structures of the phenyl-in and cyclohexyl-in complexes are stabilized mainly by hydrophobic interactions. The effective distances calculated based on the SA structures are close to those for the MM structures. Because the plot of $ROE/n_{CD}n_{OB}$ against d_{eff} for the SA structures is close to Fig. 6, the data are not shown.

Conformational Changes of OB with α-CD Inclusion. Based on NMR measurements and calculations of the molecular mechanics, molecular dynamics, and molecular surface areas, we determined the structure of OB in an aqueous solution.[5] The chemical shifts of the cyclohexyl protons are

very sensitive to the configuration of the phenyl group, namely, to the dihedral angles (φ_1 and φ_2) as defined in Fig. 1. OB has four pairs of corresponding protons (H2a and H6a, H2e and H6e, H3a and H5a, and H3e and H5e). As Table 1 shows, the chemical shifts of the paired protons are different from one another. This magnetic nonequivalence was ascribed to the difference in the ring-current effects of the phenyl group on the paired protons.[5] The observed chemical-shift differences ($\Delta\delta$) for four pairs of the protons were best fitted to those calculated based on the ring-current effect by regarding the dihedral angles as being adjustable parameters to determine the structure of OB in the free state.[5–7,22,26,28] This NMR structure is shown by the light lines of Fig. 9. The fitness of the chemical shifts was judged from the magnitude of SS. These best-fit values are given in Table 5.

This procedure was employed to estimate the average structure of OB in the OB–α-CD complex; we cannot separately determine the structures of OB in the phenyl-in complex and in the cyclohexyl-in complex. If the cyclohexyl group is incorporated symmetrically in the α-CD cavity, the chemical-shift variations of the paired protons on complexation will be identical. Then, the difference ($\Delta\delta$) between the chemical shifts (δ_{OB-CD}) of the paired protons is caused by the ring-current effect alone. This difference is shown for four pairs in Table 5. These observed chemical-shift differences ($\Delta\delta$) for four pairs of the protons were best fitted to those calculated based on the ring-current effect by regarding the dihedral angles as being adjustable parameters. This structure of the complex is shown by the dark lines of Fig. 9, and is less crowded than that of the free OB molecule (light lines). This induced structural change facilitates the complexation of OB with α-CD.

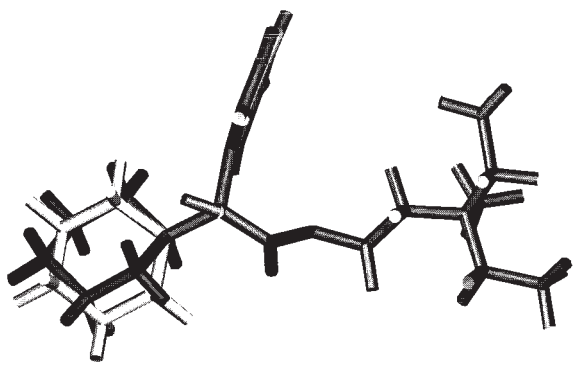

Fig. 9. Three-dimensional structures of OB in the free state (light lines) and in the complex (dark lines) estimated from NMR chemical shifts.

The dihedral angles (φ_1 and φ_2) of OB in the complex determined by molecular mechanics are given in Table 4. The average dihedral angle is connected with those of the two complexes as:

$$\varphi_1 = (K_{1C}\varphi_{1C} + K_{1P}\varphi_{1P})/K_1, \quad (12)$$

$$\varphi_2 = (K_{1C}\varphi_{2C} + K_{1P}\varphi_{2P})/K_1, \quad (13)$$

where $\varphi_{1C} = -59^\circ$, $\varphi_{1P} = -76^\circ$, $\varphi_{2C} = 56^\circ$, and $\varphi_{2P} = 65^\circ$. Though there are some uncertainties in the estimation of K_{1C} and K_{1P} (see Discussion Section), the values of φ_1 and φ_2 estimated by molecular mechanics are close to those estimated by NMR (Table 5). Thus, φ_2 does change significantly upon complexation, though φ_1 remains unchanged. The decrease in φ_2 facilitates the complexation of OB into the α-CD cavity.

Discussion

Chemical Shifts and Binding Constants. The chemical-shift change ($\Delta\delta_{OB-CD}$) with complexation has not been used very much for determining the structure of the complex.[6,7,26] To determine this value accurately, we must pay special attention to chemical-shift references. The chemical shift in reference to an external standard changed linearly with increasing CD concentration.[16,18,29,30] To determine the binding constant, we must correct this change.[29,30] Internal reference compounds are often bound to CD and guest molecules by hydrophobic and electrostatic interactions.[16,29,30] To avoid these complications, we employed tetramethylammonium chloride as an inert, internal reference.[16] Using the chemical shift for the OB–α-CD system, we determined reasonable binding constants and estimated the structures of the OB–α-CD complexes. Although ESR and time-resolved fluorescence spectroscopies had detected two types of 1:1 complexes, they had not given detailed information on these structures.[10–12]

Regardless of the kinds of guests and cyclodextrins, the ΔA_{oo} value is correlated with the binding constant at 298 K as[18]

$$\log K_1 = 1.803\Delta A_{oo} - 2.323. \quad (14)$$

Using Eq. 14 with the ΔA_{oo} values shown in Table 4, we can estimate the microscopic binding constants for the phenyl-in and cyclohexyl-in complexes, as shown in Table 4. The macroscopic binding constant estimated from the SA structure is 50.7 M^{-1}, whereas the value estimated from the MM structure is 28.8 M^{-1}. The theoretical binding constant estimated from the SA structure is closer to the observed value (70

Table 5. Observed and Calculated Chemical Shift Differences between a Pair of Protons and the Dihedral Angles around the C1–C* and C(phenyl)–C* Bond Axes for Free and Complexed OB

Paired proton	Free OB					Complexed OB				
	$\Delta\delta_{OBobsd}$	$\Delta\delta_{OBcalcd}$	φ_1	φ_2	SS[a)]	$\Delta\delta_{OB-CDobsd}$	$\Delta\delta_{OB-CDcalcd}$	φ_1	φ_2	SS
H6e–H2e	−0.152	−0.150				−0.388	−0.432			
H6a–H2a	−0.378	−0.350				−0.155	−0.107			
H5e–H3e	−0.026	−0.021				−0.196	−0.066			
H5a–H3a	−0.140	−0.122				−0.149	−0.118			
			−64°	102°	0.001			−61°	67°	0.022

a) $SS = \sum(\delta_{calcd} - \delta_{obsd})^2$

M^{-1}) than that from the MM structure.

Estimation of the Molar Ratio of Two Complexes. Table 2 compiles the binding constants of phenol[31–36] and cyclohexanol[27,32,37,38] with α-CD at 298 and 308 K. Among these values, the binding constants determined by Gelb et al. at 298 K seem to be the most reasonable for phenol and cyclohexanol.[32,39] They obtained binding constants of 19.8 and 56 M^{-1} for phenol and cyclohexanol at 308 K. If we employ these values for the phenyl-in and cyclohexyl-in complexations in the equation $K_1 = K_{1p} + K_{1c}$, we can estimate a binding constant of 75.8 M^{-1} for OB. This is very close to our value for OB obtained by NMR (Table 2).[40] This agreement also supports the coexistence of two kinds of complexes of OB and α-CD, and allows us to estimate the mole fractions of these complexes; the mole fractions of the phenyl-in and cyclohexyl-in complexes are 0.3 and 0.7, respectively.

The other estimation of the molar ratio of the two complexes comes from a comparison of the $\Delta\delta_{OB-CD}$ values of OB with those of BS.[23] As Table 1 shows, the $\Delta\delta_{OB-CD}$ values for Ho, Hm, and Hp of OB are smaller than those for the BS–α-CD complex. The $\Delta\delta_{OB-CD}$ values of the phenyl protons for the cyclohexyl-in complex would be assumed to be zero in Eq. 11. Then, because $\Delta\delta_{OB-CDC} = 0$, the mole fraction of the phenyl-in complex is $K_{1P}/K_1 = \Delta\delta_{OB-CD}/\Delta\delta_{OB-CDP}$. Because the geometry of the phenyl group in the phenyl-in complex (Figs. 6a and 6c) is close to that in the BS complex (Fig. 3d in Ref. 26), the $\Delta\delta_{OB-CDP}$ values of the phenyl protons for the phenyl-in complex would be assumed to be equal to those for the BS–α-CD complex in Eq. 11. Therefore, the ratio of $\Delta\delta_{OB-CD}$(OB) to $\Delta\delta_{complex}$(BS) gives an estimation of the mole fraction of the phenyl-in complex: 0.23 for Ho, 0.56 for Hm, and 0.36 for Hp. The average of these mole fractions is 0.38. This value is similar to the mole fraction of 0.3 estimated from the binding constants.

The $ROE/n_{CD}n_{OB}$ value should increase as the concentration of the OB–α-CD complex increases. As shown in Fig. 7, the $ROE/n_{CD}n_{OB}$ value for the cyclohexyl-in complex is slightly larger than that for the phenyl-in complex. This finding is consistent with the molar ratios estimated from the binding constants and chemical shifts.

Implications of the Present Work. In this work we used a racemic mixture of *R*- and *S*-OB, but analyzed the *S*-form alone. Because the binding sites of OB to α-CD are the phenyl and cyclohexyl groups, the difference in α-CD inclusion between *R*- and *S*-OB would be slight. In fact, we failed to separate this racemic mixture with α-CD by a few methods (unpublished results).

Electromotive-force measurements established the 1:1 stoichiometry of OB and α-CD.[4] OB has two binding sites, the phenyl and cyclohexyl groups. Because these groups are very crowded, OB cannot form the 1:2 complex of OB to α-CD.

Though molecular surface areas have been used to estimate the aqueous solubility, the partition coefficient, critical micelle concentrations, HPLC retention times, bioactivity, and the molecular conformation,[8,18] they have been applied only a little to docking studies.[18,26] This approach will be applied to other host-guest systems.

Thanks are due to the late Dr. Sakae Hada and Mr. Ryusaku Kawaguchi for preliminary experiments. The work is supported by Grants-in-Aid from the Scientific Research Program (No. 116721153) and the Frontier Research Program of the Ministry of Education, Science, Sports and Culture.

References

1 M. L. Bender and M. Komiyama, "Cyclodextrin Chemistry," Springer-Verlag, Berlin (1978), Chaps. 2 and 3.

2 J. Szejtli, "Cyclodextrin Technology," Kluwer Academic Publishers, Dordrecht (1988), Chaps. 1 and 3.

3 N. Funasaki, R. Kawaguchi, S. Hada, and S. Neya, *J. Pharm. Sci.*, **88**, 759 (1999).

4 N. Funasaki, R. Kawaguchi, S. Ishikawa, S. Hada, S. Neya, and T. Katsu, *Anal. Chem.*, **71**, 1733 (1999).

5 N. Funasaki, H. Yamaguchi, S. Ishikawa, and S. Neya, *J. Phys. Chem. B*, **104**, 10412 (2000).

6 Y. Inoue, *Ann. Rep. NMR Spectrosc.*, **27**, 60 (1993).

7 H.-J. Schneider, F. Hacket, V. Rüdiger, and H. Ikeda, *Chem. Rev.*, **98**, 1755 (1998).

8 S. Ishikawa, S. Neya, and N. Funasaki, *J. Phys. Chem. B*, **102**, 2502 (1998).

9 H. Dodziuk, J. Sitkowski, L. Stefaniak, D. Sybilska, and J. Jurczak, *Supramol. Chem.*, **7**, 33 (1996).

10 Y. Kotake and E. G. Janzen, *J. Am. Chem. Soc.*, **110**, 3699 (1988).

11 Y. Kotake and E. G. Janzen, *J. Am. Chem. Soc.*, **111**, 7319 (1989).

12 A. Nakamura, K. Saitoh, and F. Toda, *Chem. Lett.*, **1989**, 2209.

13 K. A. Connors and D. D. Pendergast, *J. Am. Chem. Soc.*, **106**, 7607 (1984).

14 K. A. Connors, *Chem. Rev.*, **97**, 1325 (1997).

15 N. Funasaki and S. Neya, *Langmuir*, **16**, 5343 (2000).

16 Y. Matsui and S. Tokunaga, *Bull. Chem. Soc. Jpn.*, **69**, 2477 (1996).

17 K. Harata, *Bull. Chem. Soc. Jpn.*, **49**, 2066 (1976).

18 S. Ishikawa, S. Hada, S. Neya, and N. Funasaki, *J. Phys. Chem. B*, **103**, 1208 (1999) and references therein.

19 Insight II version 98, San Diego, Biosystem Technologies, 1998.

20 A. Bondi, *J. Phys. Chem. B*, **68**, 441 (1964).

21 D. J. Wood, F. E. Hruska, and W. Saenger, *J. Am. Chem. Soc.*, **99**, 1735 (1977).

22 S. Hada, S. Ishikawa, S. Neya, and N. Funasaki, *J. Phys. Chem. B*, **103**, 2579 (1999).

23 H.-J. Schneider and A. Yatsimirsky, "Principles and Methods in Supramolecular Chemistry," John Wiley and Sons, Chichester, England (2000), Chap. D.

24 H. Kessler and S. Seip, "Two-dimensional NMR Spectroscopy," 2nd ed, ed by W. R. Croasmun and R. M. K. Carlson, Wiley-VCH, New York (1994), Chap. 5.

25 D. Neuhaus and M. P. Williamson, "The Nuclear Overhauser Effect in Structural and Conformational Analysis," 2nd ed, Wiley-VCH, New York (2000), Chap. 12.

26 N. Funasaki, H. Yamaguchi, S. Ishikawa, and S. Neya, *J. Phys. Chem. B*, **105**, 760 (2001).

27 M. V. Rekharsky, F. P. Schwartz, Y. B. Tewari, R. N. Goldberg, M. Tanaka, and Y. Yamashoji, *J. Phys. Chem.*, **98**, 4098 (1994).

28 F. A. Bovey, "Nuclear Magnetic Resonance Spectro-

scopy,'' Academic Press, New York and London (1969), Chap. 3, and Appendix C. C. E. Johnson, Jr. and F. A. Bovey, *J. Chem. Phys.*, **29**, 1012 (1958).

29 N. Funasaki, M. Nomura, H. Yamaguchi, S. Ishikawa, and S. Neya, *Bull. Chem. Soc. Jpn.*, **73**, 2727 (2000).

30 N. Funasaki, M. Nomura, S. Ishikawa, and S. Neya, *J. Phys. Chem. B*, **105**, 7361 (2001).

31 G. L. Bertrand, J. R. Faulkner, Jr., S. M. Han, and D. W. Armstrong, *J. Phys. Chem.*, **93**, 6863 (1989).

32 R. I. Gelb, L. M. Schwartz, M. Radeos, R. B. Edmonds, and D. A. Laufer, *J. Am. Chem. Soc.*, **104**, 6283 (1982).

33 R. Breslow and P. Campbell, *Bioorg. Chem.*, **1**, 140 (1971).

34 E. A. Lewis and L. D. Hansen, *J. Chem. Soc., Perkin Trans. 2*, **1973**, 2081.

35 R. L. van Etten, J. F. Sebastian, G. A. Clowes, and M. L. Bender, *J. Am. Chem. Soc.*, **89**, 3242 (1967).

36 S.-F. Lin and K. A. Connors, *J. Pharm. Sci.*, **72**, 1333 (1983).

37 Y. Matsui and K. Mochida, *Bull. Chem. Soc. Jpn.*, **52**, 2808 (1979).

38 S. Takagi and M. Maeda, *J. Inclusion. Phenomena*, **2**, 775 (1984).

39 A reliable binding constant will be a value close to one another among the values determined by many researchers and different methods. According to this criterion, the binding constants for phenol and cyclohexanol at 298 K, determined by Gelb et al., are reliable values.[32] Therefore, those values at 307 K determined by them were regarded as reliable ones.

40 Table 2 demonstrates that the binding constant is dependent on researchers, methods, and experimental conditions (salt concentration, temperature, and solvent H_2O or D_2O). Because the present agreement is beyond the accuracy of binding constant determination, it should not be overestimated.